The Astrophysical Journal Letters, 745:L24 (6pp), 2012 February 1 doi:10.1088/2041-8205/745/2/L24

DISSECTING EARLY-TYPE DWARF GALAXIES INTO THEIR MULTIPLE COMPONENTS

J. Janz[1,2,11], E. Laurikainen[1,3], T. Lisker[2], H. Salo[1], R. F. Peletier[4], S.-M. Niemi[5], M. den Brok[4], E. Toloba[6], J. Falcón-Barroso[7,8], A. Boselli[9], and G. Hensler[10]

[1] Division of Astronomy, Department of Physics, University of Oulu, P.O. Box 3000, FI-90014 Oulun Yliopisto, Finland; jjanz@ari.uni-heidelberg.de
[2] Astronomisches Rechen-Institut, Zentrum für Astronomie der Universität Heidelberg, Mönchhofstraße 12-14, D-69120 Heidelberg, Germany
[3] Finnish Centre for Astronomy with ESO (FINCA), University of Turku, Turku, Finland
[4] Kapteyn Astronomical Institute, University of Groningen, P.O. Box 800, 9700 AV Groningen, The Netherlands
[5] Department of Physics and Astronomy, University of North Carolina, Chapel Hill, CB 3255, Phillips Hall, Chapel Hill, NC 27599-3255, USA
[6] UCO/Lick Observatory, University of California, Santa Cruz, 1156 High Street, Santa Cruz, CA 95064, USA
[7] Instituto de Astrofísica de Canarias, Vía Láctea s/n, La Laguna, Tenerife, Spain
[8] Departamento de Astrofísica, Universidad de La Laguna, E-38205 La Laguna, Tenerife, Spain
[9] Laboratoire d'Astrophysique de Marseille, UMR 6110 CNRS, 36 rue F. Joliot-Curie, F-13388 Marseille, France
[10] Institute of Astronomy, University of Vienna, Türkenschanzstraße 17, 1180 Vienna, Austria
Received 2011 November 1; accepted 2011 December 19; published 2012 January 10

ABSTRACT

Early-type dwarf galaxies, once believed to be simple systems, have recently been shown to exhibit an intriguing diversity in structure and stellar content. To analyze this further, we started the *SMAKCED* project (Stellar content, MAss and Kinematics of Cluster Early-type Dwarfs, http://www.smakced.net) and obtained deep *H*-band images for 101 early-type dwarf galaxies in the Virgo Cluster in a brightness range of $-19\,\mathrm{mag} \leqslant M_r \leqslant -16$ mag, typically reaching a signal-to-noise ratio of 1 per pixel of $\sim 0\farcs25$ at surface brightnesses $\sim$22.5 mag arcsec^{-2} in the *H* band. Here we present the first results of decomposing their two-dimensional light distributions. This is the first study dedicated to early-type dwarf galaxies using the two-dimensional multi-component decomposition approach, which has been proven to be important for giant galaxies. Armed with this new technique, we find more structural components than previous studies: only a quarter of the galaxies fall into the simplest group, namely, those represented by a single Sérsic function, optionally with a nucleus. Furthermore, we find a bar fraction of 18%. We also detect a similar fraction of lenses which appear as shallow structures with sharp outer edges. Galaxies with bars and lenses are found to be more concentrated toward the Virgo galaxy center than the other sample galaxies.

Key words: galaxies: clusters: individual (Virgo Cluster) – galaxies: dwarf – galaxies: elliptical and lenticular, cD – galaxies: photometry – galaxies: structure

Online-only material: color figures

1. INTRODUCTION

Early-type dwarf (dE) galaxies are the most abundant galaxy population in high-density environments. Their low mass and large number make them ideal probes of the mechanisms that can alter the appearance of galaxies: internal processes as well as environmental influences. Their ubiquity and susceptibility to various physical mechanisms give them a key role in understanding galaxy cluster evolution. The popular belief that dEs were formed from spiral and irregular galaxies at late epochs by the cluster environment (e.g., Moore et al. 1998; Boselli et al. 2008; Kormendy & Bender 2012; Toloba et al. 2011) is contrasted with the formation of dEs in models of a ΛCDM universe, as the descendants of cosmological building blocks. In the latter scenario dEs would be close relatives to their giant counterparts (e.g., de Rijcke et al. 2005; Janz & Lisker 2008, 2009; Weinmann et al. 2011).

Disk structures in dEs have been searched for since the early 1990s (Binggeli & Cameron 1991; Jerjen et al. 2000; Barazza et al. 2002). The prevailing interpretation was that the disk structures, as imprints of their host galaxy's history, point at late-type disk galaxies as progenitors for dEs. Subsequent work in recent years has shown that dEs are rather heterogeneous, with their various characteristics depending strongly on the position within the cluster: different subclasses based on morphology and stellar population characteristics were identified (Lisker et al. 2006a, 2006b, 2007, 2008); dEs are not old in general, but cover a large range in age and metallicity (Michielsen et al. 2008; Paudel et al. 2010); the degree of rotational support varies (Toloba et al. 2009, 2011); and their shapes seem to depend even on their orbital characteristics (Lisker et al. 2009). The various results imply that the dEs might be a mixed bag, possibly with multiple formation channels (Lisker 2009).

Here, we explore the feasibility of revealing detailed structures in dEs using a two-dimensional multi-component decomposition approach. Laurikainen et al. (2010) demonstrated for S0s how morphological information via such detailed decompositions can contribute to unveiling possible formation processes of those galaxies. Surprisingly, we find that only a minority of the dEs in the Virgo Cluster appears to follow the classical picture of a featureless galaxy.

2. DATA

Within the *SMAKCED* project[12] we aim at obtaining deep *H*-band images for a complete sample of 174 early-type galaxies in the Virgo Cluster in the brightness range of $-19\,\mathrm{mag} \leqslant M_r \leqslant -16$ mag ($[m - M]_{\mathrm{Virgo}} = 31.09$ mag; Mei et al. 2007). The sample is drawn from the Virgo Cluster catalog (VCC; Binggeli et al. 1985, "certain members"). Observations in the

[11] Fellow of the Gottlieb Daimler and Karl Benz Foundation

[12] Stellar content, MAss and Kinematics of Cluster Early-type Dwarfs, http://www.smakced.net

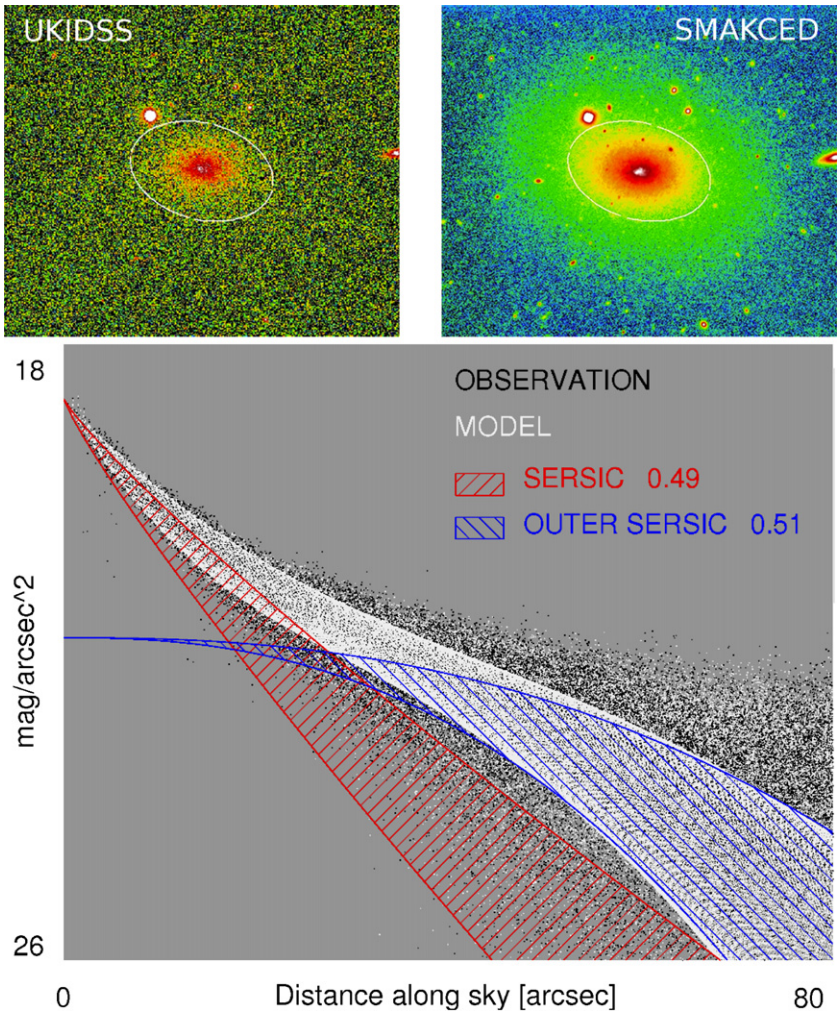

Figure 1. One example (VCC0170) of the observed two-dimensional light profiles with the fitted components. The observation (every unmasked pixel in the image) is displayed with black points, the total model in white, and the individual components with shaded areas. The numbers quote the fractions of light in the components. For a direct comparison with the observation the model is plotted twice: the pure model is the white band with well-defined boundaries. For another illustration of the model (white dots spread among the black dots of the observation) random values were added according to the noise in the observed image. For clarity, the nuclear component, which is slightly offset in this galaxy, is not plotted. Top panels show the UKIDSS NIR image (left) and our image obtained with ESO NTT (right). The optical half-light radius ($r_e = 32''$; Janz & Lisker 2008) is indicated with an ellipse. North is left.

(A color version of this figure is available in the online journal.)

near-infrared (NIR) allow the most direct characterization of the galaxies' stellar mass distribution and are much less affected by dust extinction than in the optical. Some dEs contain dust (Peletier 1993; Lisker et al. 2006b; de Looze et al. 2010), which could mimic complex structures. During 2010–2011 we obtained images for 81 of the 174 galaxies with the ESO New Technology Telescope (NTT), the Telescopio Nazionale Galileo, and the Nordic Optical Telescope. Complemented with archival data this yields a sample of 101 galaxies. Our images typically reach an H-band surface brightness of 22.2–23.0 mag arcsec^{-2} at a signal-to-noise ratio (S/N) = 1 per pixel (scale 0.″234–0.″288), deeper than in previous works (Figure 1). The reductions of the on-target dithered observations, done with IRAF, included cross-talk removal, flat fielding, sky subtraction, and correction for the field distortions, where necessary.

3. TWO-DIMENSIONAL DECOMPOSITIONS

For decomposing the galaxies' light into potentially multiple components we employ GALFIT 3.0 (Peng et al. 2010), which uses a χ^2 minimization algorithm to find the optimal solution for a given set of functions and starting values. GALFIT's solutions were visually evaluated using GALFIDL,[13] a set of IDL routines. Fore- and background sources were masked out; the point-spread function (PSF) FWHM was determined for several point-like sources using SExtractor on each image (typically ∼0.″9) and the model was convolved with the averaged (Gaussian) PSF during the fitting process.

As further input GALFIT needs the uncertainties of the pixel values, i.e., a σ-image. We calculate, for each pixel, the standard deviation over the individual images, taking advantage of the large number of exposures for each galaxy. The obtained σ-image is normalized to correspond to the sky pixel-to-pixel variations in the final co-added image. The model fitting does not incorporate possible systematic large-scale background variations. The potential bias by such variations is estimated from the rms of mean sky values in small boxes distributed on the image. Such a bias could alter the profiles within the shaded area indicated in Figure 2.

[13] H. Salo, http://sun3.oulu.fi/∼hsalo/galfidl.html

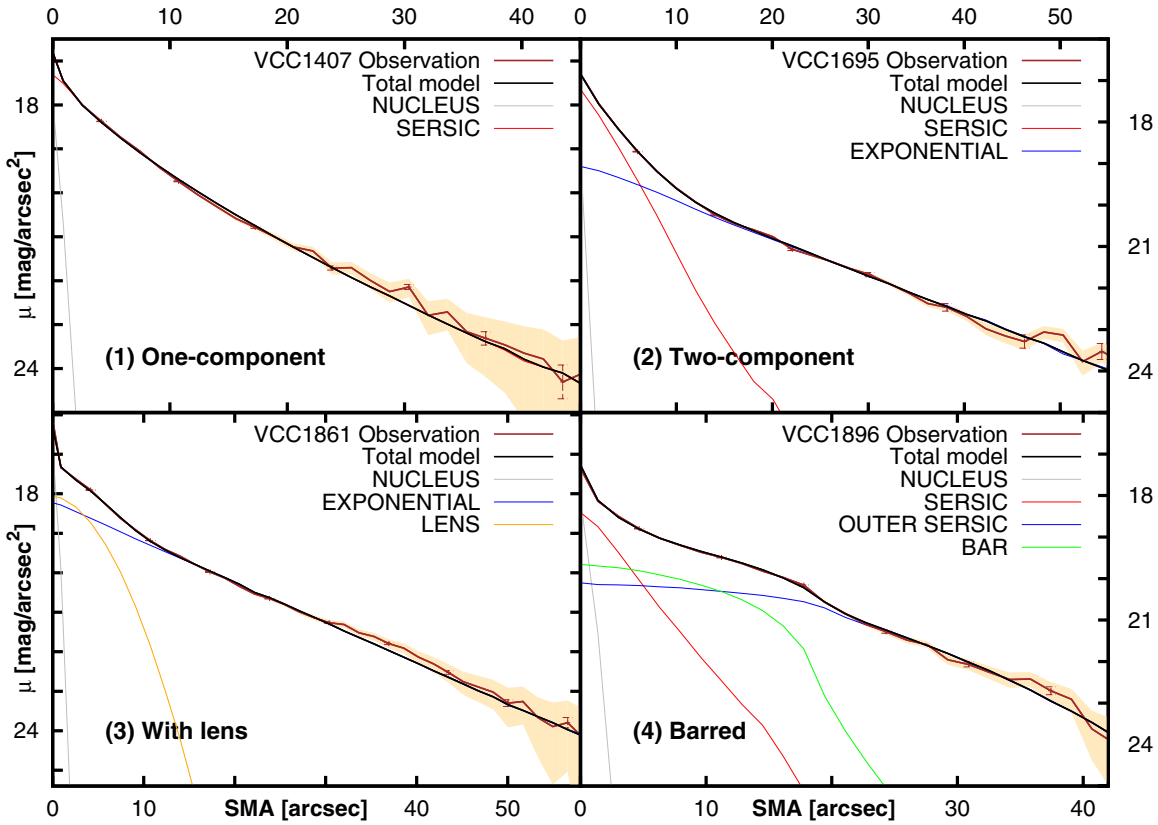

Figure 2. Groups of structural types. We identified four characteristic, distinct structural types by decomposing the two-dimensional light distributions of the galaxies (see Section 4.1). The panels show light profiles for representative galaxies (SMA = semimajor axis). The shaded areas display the maximal systematic error, estimated by adding and subtracting the large-scale background variations' rms to the intensities. The error bars indicate the intensity uncertainties as measured by IRAF/`ellipse`.

(A color version of this figure is available in the online journal.)

For all galaxies we fitted the following basic models: one-component, one-component+nucleus, and two-component models. Sérsic (1963) functions were used for the components, while the nucleus was modeled by a point source. Subsequently, we visually evaluated the quality of the fit by inspecting the residual structures seen in the model-subtracted images (Figure 3) and in profile representations showing all observed pixels (Figure 1). We also inspected the one-dimensional surface brightness profiles and profiles of position angle and ellipticity (obtained by IRAF/`ellipse` fitting). When deemed necessary from the fit residuals and profile representations, we fitted models with additional bar or lens components. Lens, in this context, refers to an inner component with "a shallow brightness gradient with a sharp outer edge" (Kormendy 1979). In distinction to bars ($b/a \lesssim 0.5$), lenses have intrinsic axial ratios close to unity ($b/a > 0.7$).

The basic models consist of one or two Sérsic functions. The fit of the outer component in the two-component model had a Sérsic index n fixed to 1 (i.e., exponential). Its orientation and ellipticity were fixed to the mean of the outer isophotes. For a few galaxies n was a free parameter, to account for a steeper drop of the outer profile with $n < 1$ (Figure 1 and panel 4 of Figure 2). For a substantial number of the two-component galaxies, the Sérsic index of the inner component is $n \approx 1$ ($n < 1.2$ for 53%). For bars and lenses we chose Ferrers' function (see Peng et al. 2010) with elliptical isophotes, since it allows for a better treatment of the outer cutoff of the surface brightness (see Laurikainen et al. 2009). In a few cases the fit was considerably improved when the center for each component was left free. Notably most of those galaxies were classified as having residual star formation in the center (dE(bc)s; Lisker et al. 2006b).

4. RESULTS

4.1. Groups of Structural Types

We order the galaxies by the set of components building up the galaxy's model and define the following groups: (1) one component, (2) two components (typically Sérsic+exponential), (3) galaxies with lenses, and (4) barred galaxies. Representative examples for the groups are shown in Figure 2. The final model for a given galaxy, and thus its group assignment, was chosen based on the visually judged improvement of the residual structures (Figure 3) and profile representations.

In most cases the lens is accompanied by an exponential outer component; however, in two cases it is a Sérsic component with $n > 1$. Only three of the galaxies with a lens have three components (not counting the nucleus). The galaxies with lenses might be regarded as two-component systems with further complexity (cf. Binggeli & Cameron 1991), but we assign them to their own group. The presence of a nucleus does not affect the group designation. For in-depth analysis of nuclei in dEs we refer to the literature, especially to studies resolving them (i.e., Advanced Camera for Surveys (ACS), Virgo Cluster Survey; Ferrarese et al. 2006). Spiral arms can be clearly seen in the residual image of four galaxies, while for two more galaxies they are at the detection limit. Two of the galaxies with a lens additionally host a small bar.

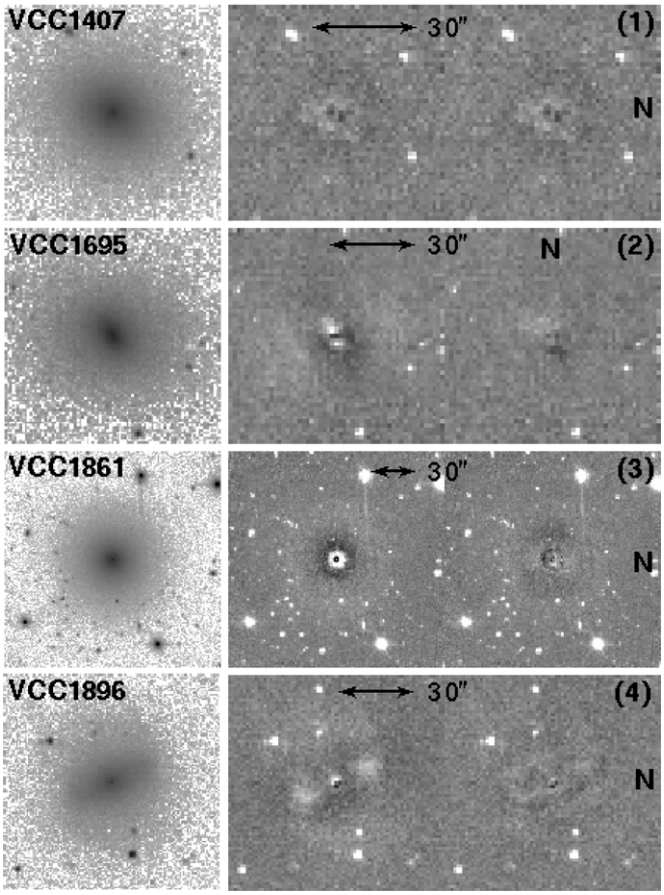

Figure 3. Comparison of simple and final models for the galaxies in Figure 2. In each row we show a cutout of the galaxy image (left), as well as the residuals after subtracting a simple Sérsic+nucleus (middle) and the final model (right). The gray scales show $\pm 3\sigma$ for the residual images; north is the direction indicated by *N*.

It is not possible to assign all galaxies unambiguously to one group, since two different models might fit equally well. Uncertainties that would shift the galaxies from the two- to one-component group include: (a1) the improvement of two components over the one-component model is marginal and (a2) the inner component of a galaxy fitted by a Sérsic function is so small that it might be just a nuclear component. If the edge of a lens is less well defined, the component can be alternatively fitted with a Sérsic function with $n < 1$, which would shift the galaxy from the group with lenses to the two-component group (b). Bars are characterized by high ellipticity and possibly an orientation distinct from the disk component, but they are modeled with the same function as lenses. Especially in more inclined galaxies this distinction can become difficult, the less certain cases being listed as (c).

In Table 1 we summarize the number statistics for the four groups and number the less certain cases among them. The sample is divided into different bins of galaxy brightness, morphological subclass, and projected clustercentric distance.[14] In total 22 galaxies are not included in any group as their decomposition is unreliable: 14 are more inclined than 65°, i.e., axis ratio $< \cos(65^\circ)$, and for 8 galaxies no satisfactory fit was achieved due to persistent residuals structures.

[14] We consider the cluster center to be marked by M87.

4.2. Analysis

First and foremost our analysis separates galaxies that satisfy the simplest one-component models from those with more complex structures. The fraction of simple galaxies is surprisingly low, given the picture of dEs as structureless, red and dead galaxies: only 24% of the galaxies in our analyzed sample exhibit a simple structure (see Table 1, 27% of those with dE classification; 34% when adding the less certain two-component galaxies). Obviously, our low fraction of simple galaxies might even decrease if still deeper images were available.

The largest fractions of simple galaxies are found among those where no disk feature or blue center had been identified previously (Lisker et al. 2007), and among the faintest galaxies. That the fraction of galaxies with multi-component structures increases toward brighter galaxies in Table 1 is not a simple selection effect, since the desired image depth was chosen according to the surface brightness at the half-light radius of each galaxy. Therefore, we do not expect to miss components in dimmer galaxies provided that they contain a similar fraction of light and have similar relative extent. While galaxies of higher mass may be expected to shield their structures more easily against external heating, the increase of the multi-component galaxy fraction with increasing galaxy brightness is not statistically significant: a Kolmogorov–Smirnov (K-S) test yields 7.2% probability for them being drawn from the same brightness distribution.

Figure 4 displays the distribution of galaxies in the different groups inside the Virgo Cluster. Simple galaxies appear less centrally concentrated (see also Table 1), but the clustercentric distances of simple and multi-component galaxies do not differ significantly according to a K-S-test. Indeed, simple galaxies are distributed similarly to two-component galaxies, which constitute the major part of the multi-component ones. On the other hand, barred galaxies are more concentrated toward the projected cluster center than the two-component galaxies (K-S-test 1.6%; 4.6% when comparing barred and one-component galaxies).

Bars were fitted in 12 galaxies, 4 of them being classified as less certain. With the two small bars in galaxies *with lenses*, not fitted in the decompositions, this leads to a bar fraction of 18% (13% without less certain cases). Some galaxies in our sample fall into the dwarf brightness regime, but were previously classified as E or S0. Omitting these galaxies does not change the bar fraction. Lenses were fitted in 14 galaxies (18%). Kormendy (1979) suggested that bars and lenses are evolutionary related, i.e., that lenses are dissolved bars. When we treat barred galaxies and galaxies with a lens as one combined group, we find their projected clustercentric distance distribution to be significantly different from that of the other dEs (K-S-test 0.4%).

5. DISCUSSION

Recent studies of detailed structures in the dEs in the Virgo Cluster include McDonald et al. (2011), Ferrarese et al. (2006), and Lisker et al. (2006a). McDonald et al. (2011) fitted Sérsic and Sérsic+exponential models to the one-dimensional light profiles of galaxies in the Virgo Cluster, also in the *H* band. Number statistics of structural components were not given, but taking their decompositions for our sample leads to a very similar fraction of simple galaxies. The agreement in a one-by-one comparison for the galaxies in common is less good, however. A fair comparison for individual cases is hindered, since the algorithm by which their fitting code decides in

Table 1
Frequencies of Structural Types

Group Less Certain Cases	1 One Component	2 Two Component (a1+a2)	3 W. Lens (b)	4 Barred (c)	Total Analyzed	Complete Sample
All	19/24%	34 (7)/43%	14 (5)/18%	12 (4)/15%	79	174
$-19 \leqslant M_r \leqslant -18$	1/8%	5 (0)/38%	4 (3)/31%	3 (0)/23%	13	28
$-18 < M_r \leqslant -17$	10/21%	23 (5)/49%	7 (1)/15%	7 (4)/15%	47	61
$-17 < M_r \leqslant -16$	8/42%	6 (2)/32%	3 (1)/16%	2 (0)/11%	19	85
dE(all)	18/27%	29 (5)/43%	10 (4)/15%	10 (4)/15%	67	145
dE(N)	11/37%	8 (1)/27%	8 (3)/27%	3 (2)/10%	30	106
dE(nN)	2/40%	3 (0)/60%	0	0	5	27
dE(di)	4/16%	11 (2)/44%	2 (1)/8%	8 (2)/32%	25	33
dE(bc)	1/10%	9 (2)/90%	0	0	10	15
E and S0	1/8%	5 (2)/42%	4 (1)/33%	2 (0)/17%	12	29
$D_{M87} < 1.^\circ5$	3/13%	7 (2)/30%	6 (3)/26%	7 (3)/30%	23	42
$1.^\circ5 \leqslant D_{M87} < 4^\circ$	9/26%	15 (3)/44%	6 (2)/18%	4 (1)/12%	34	84
$D_{M87} \geqslant 4^\circ$	7/32%	12 (2)/55%	2 (0)/9%	1 (0)/5%	22	48

Notes. We list numbers and fractions of galaxies in each group binned over the brightness, dE subclass (Lisker et al. 2006a, 2006b, 2007), and angular distance to M87 ($1^\circ = 0.284$ Mpc). The total sum in the subclass binning is larger than the total number of galaxies, since dEs can belong to multiple subclasses. The less certain cases in each group (a1, a2, b, and c, see Section 4.1), shown in parenthesis, are included in the numbers and fractions. Additionally, two small bars were visually identified but not fitted and therefore not counted in this table.

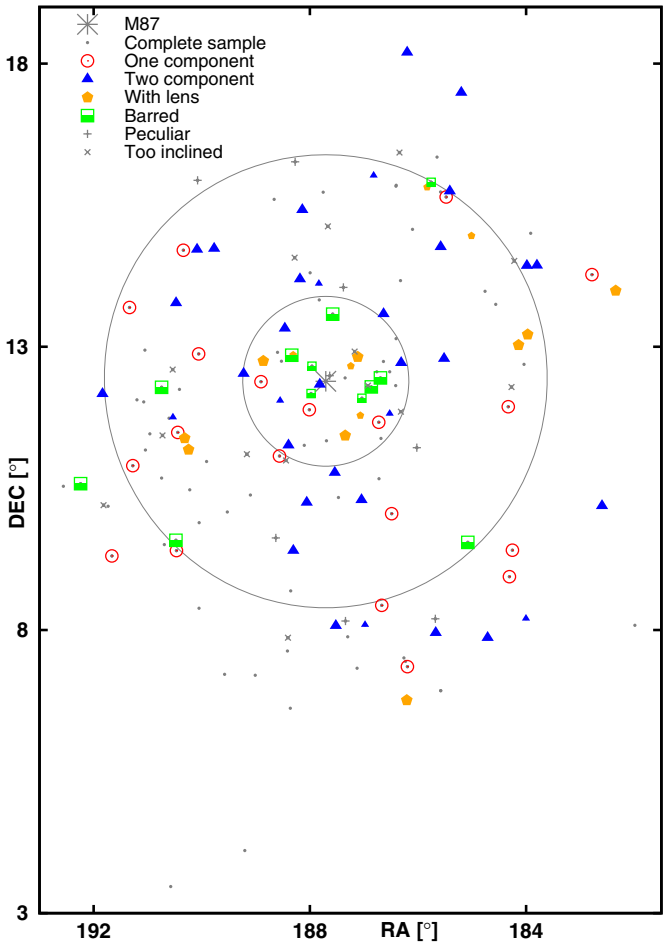

Figure 4. Distribution of the galaxies in different groups inside the Virgo Cluster. Galaxies with less certain decompositions (see Section 4.1 and Table 1) and galaxies that were not analyzed are shown with smaller symbols. The circles indicate the radial distances of $1.^\circ5$ and 4° from M87.

(A color version of this figure is available in the online journal.)

favor of one or two components has not been described in detail.

Ferrarese et al. focused more on the inner regions with the superior resolution of *Hubble Space Telescope* (*HST*) ACS. Lisker et al. (2006a) searched systematically for disk features using Sloan Digital Sky Survey images. They introduced the dE subclass named dE(di) for galaxies, in which such signatures were revealed by unsharp masking. The brightness distribution of the fraction of our galaxies fitted by more than one component is similar to their fraction of galaxies with disk features: up to 50% for the brightest dEs, but decreasing toward fainter brightnesses. Concerning morphological types, we find that 84% of the 25 dE(di)s in our sample have multiple components. In eight of them we fit a bar. Three of the four dE(di)s fitted with only one component show spiral arms in the residual images. Also, 64% of the dE(N)s in our sample (in their terminology, nucleated dEs with no other feature) show more complex morphologies. Already Binggeli & Cameron (1991) noticed visually that two-thirds of dEs in our magnitude range show a break in their *B*-band surface brightness profile, but recent studies did not take this up.

Aguerri et al. (2005) decomposed the azimuthally averaged light profiles for 99 dEs in the Coma Cluster, in a magnitude range of $-16 \leqslant M_B \leqslant -18$ mag. Their criterion for the need of two components (Sérsic+exponential; also see Graham & Guzmán 2003) was a deviation of more than 0.15 mag of the simple Sérsic model from the observed profile at any radius, taking into account photometric errors. They found that 34% of their galaxies with reliable photometry are not well fitted by a single Sérsic function. Our fraction for the Virgo Cluster is much larger, 82%, for a comparable magnitude range of $-17 \leqslant M_r \leqslant -19$ mag. It would be interesting whether the difference is due to their simpler method and worse physical resolution, or due to a real difference, for example caused by the environment. Hoyos et al. (2011) fitted single Sérsic profiles for galaxies in the Coma Cluster region using GALFIT and GIM2D on *HST*/ACS data. Since their physical resolution is comparable

to our study, their planned multi-component decompositions will provide an interesting comparison sample.

Even though Coma is more massive, denser, and has a larger fraction of red galaxies than Virgo (Weinmann et al. 2011, and references therein), the bar fraction we find in Virgo (and its decrease toward fainter galaxy brightnesses; see Table 1) agrees with the findings of Méndez-Abreu et al. (2010) for the Coma Cluster. One may speculate over the increase of the Virgo Cluster bar fraction toward the dense cluster center, and yet the similarity of the overall Virgo bar fraction to the denser Coma Cluster is due to an interplay between tidal interactions that induce bar formation and heating of the disks that impedes the formation and longevity of bars. Also bars in spiral galaxies in the Virgo Cluster (Andersen 1996), in disk galaxies in the Coma Cluster (Thompson 1981), and in clusters at intermediate redshifts (Barazza et al. 2009) were found to be more frequent toward the cluster centers.

While unsharp masking is sensitive to sharper features like bars, parametric functions fitted to the one-dimensional light profile are sensitive to deviations from a simple form, i.e., the Sérsic profile shape. Our two-dimensional fitting technique accounts for both of them in a quantitative manner. In this sense our smaller fractions of simple galaxies compared to Lisker et al. (2006a), Aguerri et al. (2005), and earlier studies may well be a consequence of the different methods used.

Paudel et al. (2010) analyzed ages and metallicities of a sample of Virgo dEs using Lick indices. They found that the dE(di)s have younger stellar populations on average than the dE(N)s (see also Toloba et al. 2009), but that also the brighter dEs, for which disk features are more frequent, have younger populations than the fainter ones. They speculate that further disks may be present in the dE(N)s but may have eluded discovery so far, which is interesting given our large fraction of galaxies with complex profiles. If late-type galaxies had been transformed into dEs (Kormendy & Bender 2012; Boselli et al. 2008), the complex structures could be understood as inherited from the progenitor. At least part of the late-type galaxies with stellar masses between $\sim 10^9$ and $\sim 10^{10}\,M_\odot$ possess a two component structure (Graham & Worley 2008). If this structure survived disk thickening, caused by tidal heating (Gnedin 2003; Smith et al. 2010) and by gas depletion from ram-pressure stripping (Smith et al. 2011), such galaxies may resemble complex dEs today.

6. SUMMARY

For the first time, we have applied a detailed two-dimensional multi-component fitting technique to a large sample of dEs, using deep NIR images. The images typically reach surface brightnesses of 22.2–23.0 mag arcsec^{-2} in the H band. In many galaxies this method has revealed more complex structures than previously known. Only for 27% of the dEs is the light distribution well represented by a single Sérsic function. Of the dE(di)s 16% were fitted by one component, but most of those appear to have disks manifested as spiral arms in the residual images. Bars were detected in 18% and lenses also in 18% of the galaxies. The physical nature of the various components remains to be investigated, ideally with a combined kinematical and stellar population analysis in future studies.

We thank H.T. Meyer, K.S.A. Hansson, and S. Paudel for helping with the observations. We thank Magnus Gålfalk and Amanda Djupvik for their kind help related to NOT. T.L. thanks Chris Flynn and Burkhard Fuchs for initiating collaborations.

J.J. acknowledges support by the Gottlieb Daimler and Karl Benz Foundation. T.L. and J.J. are supported by the German Research Foundation (DFG, GSC 129/1). H.S. and J.J. are supported by the Academy of Finland. J.F.-B. acknowledges support from the Ramón y Cajal Program and from grant AYA2010-21322-C03-02 by the Spanish Ministry of Science and Innovation.

Observations were collected at the Nordic Optical Telescope, the Telescopio Nazionale Galileo, and the European Organisation for Astronomical Research in the Southern Hemisphere (064.N-0288, 085.B-0919), based on proposals by the SMAKCED team (http://www.smakced.net).

REFERENCES

Aguerri, J. A. L., Iglesias-Páramo, J., Vílchez, J. M., Muñoz-Tuñón, C., & Sánchez-Janssen, R. 2005, AJ, 130, 475
Andersen, V. 1996, AJ, 111, 1805
Barazza, F. D., Binggeli, B., & Jerjen, H. 2002, A&A, 391, 823
Barazza, F. D., Jablonka, P., Desai, V., et al. 2009, A&A, 497, 713
Binggeli, B., & Cameron, L. M. 1991, A&A, 252, 27
Binggeli, B., Sandage, A., & Tammann, G. A. 1985, AJ, 90, 1681
Boselli, A., Boissier, S., Cortese, L., & Gavazzi, G. 2008, ApJ, 674, 742
de Looze, I., Baes, M., Zibetti, S., et al. 2010, A&A, 518, 54
de Rijcke, S., Michielsen, D., Dejonghe, H., Zeilinger, W. W., & Hau, G. K. T. 2005, A&A, 438, 491
Ferrarese, L., Côté, P., Jordán, A., et al. 2006, ApJS, 164, 334
Gnedin, O. Y. 2003, ApJ, 589, 752
Graham, A. W., & Guzmán, R. 2003, AJ, 125, 2936
Graham, A. W., & Worley, C. C. 2008, MNRAS, 388, 1708
Hoyos, C., den Brok, M., Kleijn, G. V., et al. 2011, MNRAS, 411, 2439
Janz, J., & Lisker, T. 2008, ApJ, 689, L25
Janz, J., & Lisker, T. 2009, ApJ, 696, L102
Jerjen, H., Kalnajs, A., & Binggeli, B. 2000, A&A, 358, 845
Kormendy, J. 1979, ApJ, 227, 714
Kormendy, J., & Bender, R. 2012, ApJS, 198, 2
Laurikainen, E., Salo, H., Buta, R., & Knapen, J. H. 2009, ApJ, 692, L34
Laurikainen, E., Salo, H., Buta, R., Knapen, J. H., & Comerón, S. 2010, MNRAS, 405, 1089
Lisker, T. 2009, Astron. Nachr., 330, 1043
Lisker, T., Glatt, K., Westera, P., & Grebel, E. K. 2006a, AJ, 132, 2432
Lisker, T., Grebel, E. K., & Binggeli, B. 2006b, AJ, 132, 497
Lisker, T., Grebel, E. K., & Binggeli, B. 2008, AJ, 135, 380
Lisker, T., Grebel, E. K., Binggeli, B., & Glatt, K. 2007, ApJ, 660, 1186
Lisker, T., Janz, J., Hensler, G., et al. 2009, ApJ, 706, L124
McDonald, M., Courteau, S., Tully, R. B., & Roediger, J. 2011, MNRAS, 414, 2055
Mei, S., Blakeslee, J. P., Côté, P., et al. 2007, ApJ, 655, 144
Méndez-Abreu, J., Sánchez-Janssen, R., & Aguerri, J. A. L. 2010, ApJ, 711, L61
Michielsen, D., Boselli, A., Conselice, C. J., et al. 2008, MNRAS, 385, 1374
Moore, B., Lake, G., & Katz, N. 1998, ApJ, 495, 139
Paudel, S., Lisker, T., Kuntschner, H., Grebel, E. K., & Glatt, K. 2010, MNRAS, 405, 800
Peletier, R. F. 1993, A&A, 271, 51
Peng, C. Y., Ho, L. C., Impey, C. D., & Rix, H.-W. 2010, AJ, 139, 2097
Sérsic, J. L. 1963, Bol. Asoc. Argentina Astron., 6, 41
Smith, R., Davis, J. I., & Nelson, A. H. 2010, MNRAS, 405, 1723
Smith, R., Fellhauer, M., & Assmann, P. 2011, MNRAS, in press (arXiv:1110.5555)
Thompson, L. A. 1981, ApJ, 244, L43
Toloba, E., Boselli, A., Cenarro, A. J., et al. 2011, A&A, 526, 114
Toloba, E., Boselli, A., Gorgas, J., et al. 2009, ApJ, 707, L17
Weinmann, S. M., Lisker, T., Guo, Q., Meyer, H. T., & Janz, J. 2011, MNRAS, 416, 1197